Volume 17, Issue 3, 172518 (1-11)

Iranian Journal of Earth Science (IJES)

https://doi.org/10.57647/j.ijes.2025.16863

Assessment of field displacement for implications of support design in tunneling

Naeem Abbas[1,2,*], Ke-Gang Li[1], Muhammad Zaka Emad[3], Qingci Qin[4], Mingliang Li[1], Kausar Sultan Shah[5], Rui Yue[1], Shuai Qiu[1], Khan Gul Jadoon[2]

[1]*Faculty of Land Resources Engineering, Kunming University of Science and Technology, China.*
[2]*Department of Mining Engineering Karakoram International University (KIU), Gilgit, Pakistan.*
[3]*King Fahad University of Petroleum and Minerals-KFUPM Dhahran, Kingdom of Saudi Arabia.*
[4]*Faculty of Public Security and Emergency Management, Kunming University of Science and Technology, China.*
[5]*Department of Mining and Mineral Resource Engineering, NUST, Quetta, Pakistan.*

[*]**Corresponding author:** naeem.abbas@kiu.edu.pk

Review Paper

Received:
7 March 2024
Revised:
23 May 2024
Accepted:
11 July 2024
Published online:
10 July 2025

Abstract:

In tunnel engineering, accurately predicting displacement in jointed rock masses is crucial for stability and safety. Analytical and numerical methods are commonly used to evaluate tunnel wall displacement and the effectiveness of support systems. Duncan-Fama and Carranza-Torres solutions have been employed to predict tunnel wall displacement using the ground reaction curve, both before and after support installation. A significant difference in tunnel wall displacement were observed between the two methods when the support was applied. The numerical method yielded lower displacement values compared to the analytical method. The pullout test shows the rock bolts' effective stress distribution and stability, evident through their linear stress-displacement relationship and significant yield strength expansion. The integration of both analytical and numerical methods allows for a comprehensive understanding of displacement behavior, enhancing the design and implementation of effective support systems in tunnel engineering.

Keywords: Tunneling; Support; Empirical methods; Analytical methods; Numerical modeling

1. Introduction

The stability of tunneling and underground mining relies on thorough geological investigations, the adoption of appropriate construction methods, and effective monitoring techniques. In geomechanics, analytical techniques are particularly valuable because they can provide insightful results with relatively minimal effort. These techniques highlight the critical variables influencing solutions to complex problems, thereby aiding in the prediction and management of ground behavior. The analytical methods address the challenges of predicting tunnel wall displacement in jointed rock masses (Bobet, 2010). One of the analytical method, convergence confinement in tunneling has been given to predict the tunnel wall movement using ground reaction curve (GRC) (Carranza-Torres and Fairhurst, 2000). In this method when the boundary rock moves inward, tangential stresses intensify, leading to both yielding of the rock mass and increased confining stresses on the surrounding area (Fama, 1993; Carranza-Torres and Fairhurst, 2000). The Duncan Fama Solution is one of the analytical methods to obtained the GRC and it is based on the Mohr-Coulomb failure criterion. Therefore, this method requires parameters such as modulus of elasticity (MPa), Poisson's ratio, internal friction angle, and rock mass compressive strength in order to draw the ground reaction curve. The another analytical method for tunnel stability analysis is Carranza-Torres method (Carranza-Torres and Fairhurst, 1999), which utilized the parameters of Hoek-brown.

The numerical modeling primarily depends on the nature

of the problem and the geometry of the fracture system (Jing and Hudson, 2002). For the continuum methods, there are three main approaches: The Finite Difference Method (FDM), the Finite Element Method (FEM), and the Boundary Element Method (BEM)(Bi et al., 2016). The main discrete methods include the Discrete Element Methods (DEM) and the Discrete Fracture Network (DFN) method (Jing and Hudson, 2002). Many numerical methods can be used to investigate tunnel wall displacement, such as General Particle Dynamics (Zhou et al., 2015; Bi et al., 2016; Yao et al., 2022), Peridynamics (Wang et al., 2016; Wang et al., 2017; Wang et al., 2018; Karimiazar et al., 2023) and XFEM (Zhou and Yang, 2012). Recently several reinforcement operations were simulated through numerical modeling. The findings indicate that a combination of the umbrella arch and radial grouting methods proves to be the most suitable strategy for successfully passing the Tunnel through the Lalehzar fault zone (Abdollahi et al., 2019). Numerical method helps to assess and analyze the impact of geological factors on design, as well as the reciprocal effects of design decisions on geology (Zhou et al., 2015). These are the economically feasible performances of mining applications throughout their intended operational lifespans (Singh et al., 2010). It should be noted that numerical analysis relies on available data and are dependent on the quality and representativeness of the training datasets (Hoek and Diederichs, 2006; Dehghan and Yazdi, 2023). Artificial neural networks can also rapidly and accurately predict certain aspects of numerical model results (Furtney et al., 2022). Numerical analysis aids in generating convergence curves and evaluating support response (Li et al., 2014). These solutions assume mainly elastoplastic Mohr–Coulomb behavior (Carranza-Torres, 2004) and vary primarily by their post-peak behavior, as well as modifications for other unique conditions (Hoek, 2018).

Understanding the behavior and potential impacts of faults on tunnel stability is of utmost importance to ensure safe and reliable infrastructure development (Paltrinieri et al., 2016). Zhou investigated that the tunnel stability is also dependent on pore pressure and other hydromechanical parameters (Zhao et al., 2014; Zhou et al., 2018). Zhou also used limit analysis to predict tunnel face stability in highly fractured and saturated rock masses (Zhou et al., 2017). Historical events can serve as valuable references for predicting the type of fault movement, the magnitude of displacement, and the potential occurrence of faulting in rock mass (Bao et al., 2020). This information enables the optimal and cost-effective design of structures in fault-prone areas (Öge, 2017). The basic parameter of rock mass stability analysis is rock strength and it is rock dependent (Abbas et al., 2022; Lan et al., 2019).

Given the challenges in accurately predicting displacement in highly jointed rock masses, this study compares analytical and numerical methods to evaluate tunnel wall displacement and the effectiveness of support systems. By employing the Duncan-Fama and Carranza-Torres solutions alongside numerical modeling, the research aims to provide a comprehensive understanding of displacement behavior both before and after support installation. The displacement on the recommended support has also been determined after installation the bolts using pull out test, this further confirm the validity of installed support particularly for underground excavations in highly jointed rock mass of the Himalayan.

2. The study area and the methods

The study area is situated within the Kohistan Arc, which formed as a result of the Indian and Pakistani tectonic plates beneath the Eurasian plate (Petterson, 2010). The predominant rock types in the area are Gabbronorite and ultramafic rocks. The study area is located on the border of the Khyber Pakhtunkhwa province and Gilgit-Baltistan in Pakistan, approximately 40 km downstream from Chilas, the headquarters of the Diamer district in Gilgit-Baltistan (Fig. 1. The 15.4 m span with a D-shaped tunnel is excavated on the right side of the river Indus. The tunnel passes through two different rock types according to the rock mass rating: One section has good rock mass (A), while another portion is of poor quality (B). In the poor rock mass class, the dominant rock type is ultramafic. The input parameters for the two rock types (A and B) used in the numerical analysis are provided in Table 1. The geological map of the study area is shown in Fig. 1 (Arif et al., 2015).

The Duncan Fama solution and Carranza-Torres solution are used to determine the Ground reaction Curve (GRC). The convergence is a solution typically employed for the preliminary evaluation of tunnel convergence and support suitability (Kabwe et al., 2020). The tunnel is first analyzed without support then support has been installed and the factor of safety is determined. Carranza-Torres method (Carranza-Torres and Fairhurst, 1999) integrated the Caquots lower bound solution of the problem of cavity collapse for an elastic-plastic Mohr-Coulomb material. The Carranza-Torres solution permits the estimation of the internal pressure P_s necessary to maintain the opening stability at ultimate limit state.

Stability analysis of tunnels commonly employs various approaches, namely analytical, empirical, and numerical methods. Analytical methods provide precise mathematical solutions by relying on simplifying assumptions. Empirical methods, on the other hand, are constrained by the specific conditions of their case studies. In contrast, numerical methods, such as the finite-element (FE) method, offer the capability to simulate irregular geometries and complex material models. However, the determination of ground strength parameters frequently depends on empirical methods and subjective judgment (Yang et al., 2021). An additional notable limitation of numerical modeling is its poor performance when applied beyond the range of data it has been trained on (Liu et al., 2023). This raises a fundamental question about the feasibility of extrapolating knowledge from one study to other sites and projects. The pressure exerted on tunnel support is influenced by a multitude of geological phenomena, including tectonic pressures, folds, shear zones, groundwater, and various other factors (KC et al., 2022).

The original Hoek-Brown Criterion (Hoek et al., 2002) was used in the numerical modeling. This criterion discussed is not only for rock materials. It is also applicable to

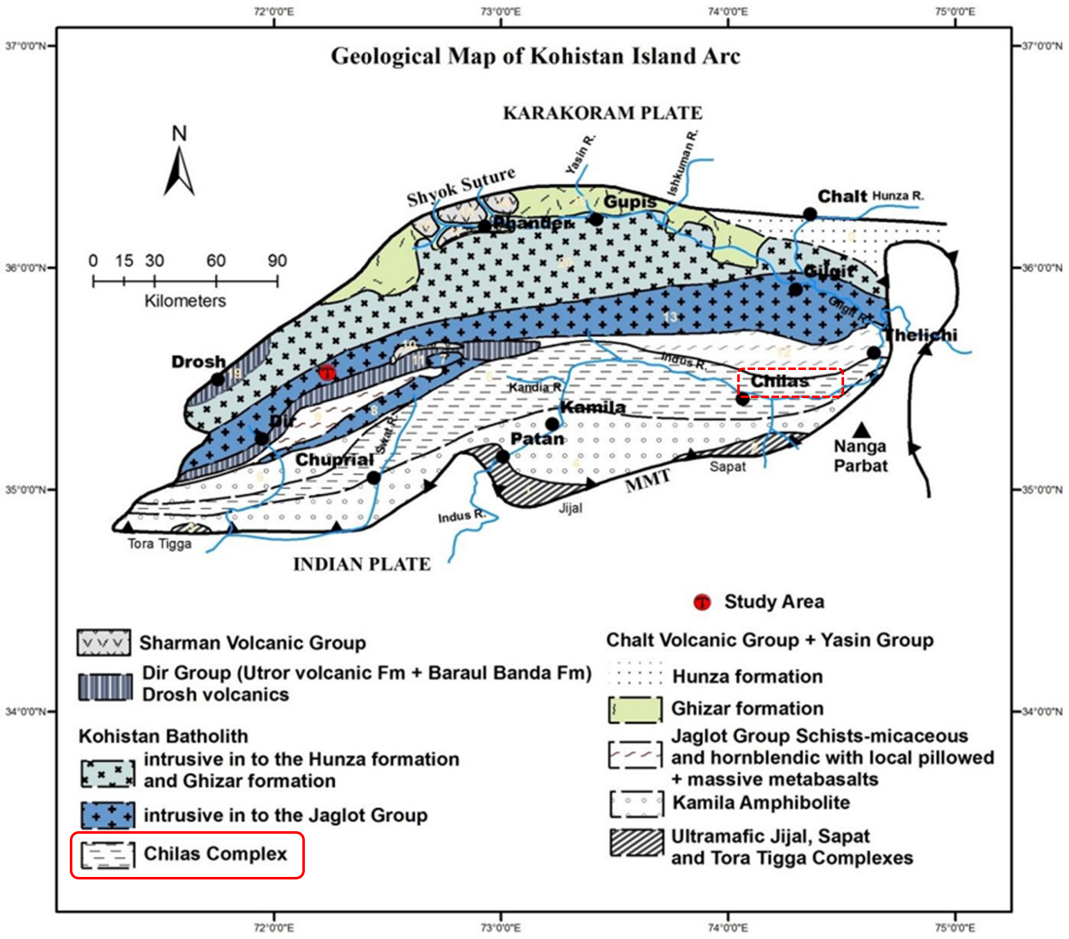

Figure 1. The geology and the location of the study area (Arif et al., 2015).

rock masses. The Hoek-brown criterion discussed for rock masses is given below,

$$\frac{\sigma_1}{\sigma_{ci}} = \frac{\sigma_3}{\sigma_{ci}} + \left(m_b \frac{\sigma_3}{\sigma_1} + s \right)^a \tag{1}$$

The equation above is the generalized Hoek-Brown criterion of rock mass. σ_1 and σ_3 are major and minor principal stresses. σ_{ci} is the unconfined compressive strength of the rock and the coefficient m_i is a parameter that depends on the type of rock (normally $5 \leq m_i \leq 40$). The Hoek-Brown criterion for intact rock material is a special form of the generalized equation when $s = 1$ and $a = 0.5$. For intact rock, m_b becomes m_i, i.e.

$$\frac{\sigma_1}{\sigma_{ci}} = \frac{\sigma_3}{\sigma_{ci}} + \left(m_i \frac{\sigma_3}{\sigma_1} + s \right)^{0.5} \tag{2}$$

In the Hoek-Brown criterion, the symbol σ_{ci} represents the uniaxial compressive strength of intact rock material. This applies both to the Hoek-Brown criterion for individual rock material and for rock masses. In the broader context of the generalized Hoek-Brown criterion, σ_1 signifies the strength of the rock mass under a confining pressure σ_3.
Parameter "a" is typically set at a value of 0.5. The constants "m_b" and "s" are parameters that vary with the type of rock and the quality of the rock mass. The specific values of "m_b" and "s" recommended by Hoek for various rock types can be found in Table 2. The input parameters of two rock types used for numerical and analytical analysis are given in Table 1.

Table 1. The properties of rock types used in numerical analysis.

Rock properties	Rock type A	Rock type B
UCS (MPa)	80	60
Unit weight	3.2	3.2
Poisson ratio	0.25	0.26
Youngs modulus (GPa)	55	50
GSI	65	55

3. Results and discussion

Rock support, plays a crucial role in tunneling projects to ensure the stability and safety of the surrounding rock mass. Wall displacement in tunneling refers to the movement or deformation of the tunnel walls during excavation (Ji et al., 2023). Using the Carranza-Torres (Fig. 2) solution the

Table 2. Relation between rock mass quality and Hoek-Brown constants (Hoek and Diederichs, 2006).

Hoek-Brown failure criterion	carbonate	lithified argillaceous rocks	arenaceous rocks	fine grained polyminerallic igneous	coarse grained polyminerallic igneous and metamorphic
Intact rock material	$m_i = 7.0$ $s = 1.0$	$m_i = 10.0$ $s = 1.0$	$m_i = 15.0$ $s = 1.0$	$m_i = 17.0$ $s = 1.0$	$m_i = 25.0$ $s = 1.0$
very good rock mass	$m_b = 3.5$ $s = 0.1$	$m_b = 5.0$ $s = 0.1$	$m_b = 7.5$ $s = 0.1$	$m_b = 8.5$ $s = 0.1$	$m_b = 12.5$ $s = 0.1$
good rock mass	$m_b = 0.7$ $s = 0.004$	$m_b = 1.0$ $s = 0.004$	$m_b = 1.5$ $s = 0.004$	$m_b = 1.7$ $s = 0.004$	$m_b = 2.5$ $s = 0.004$
fair rock mass	$m_b = 0.14$ $s = 0.0001$	$m_b = 0.20$ $s = 0.0001$	$m_b = 0.30$ $s = 0.0001$	$m_b = 0.34$ $s = 0.0001$	$m_b = 0.50$ $s = 0.0001$
poor rock mass	$m_b = 0.04$ $s = 0.00001$	$m_b = 0.05$ $s = 0.00001$	$m_b = 0.08$ $s = 0.00001$	$m_b = 0.09$ $s = 0.00001$	$m_b = 0.13$ $s = 0.00001$
very rock mass	$m_b = 0.007$ $s = 0$	$m_b = 0.01$ $s = 0$	$m_b = 0.015$ $s = 0$	$m_b = 0.017$ $s = 0$	$m_b = 0.025$ $s = 0$

ground reaction curve shows that the total wall displacement is 1.7 mm and the final wall displacement using the long term GRC is 2.55 mm without installing the support. The Carranza-Torres solution is a commonly used method for analyzing tunnel wall displacement and estimating the behavior of rock mass under the influence of tunnel excavation. The ground reaction curve obtained from this solution provides insights into the expected displacements and support requirements using Mohr Coulomb failure criteria. The total wall displacement using the Carranza-Torres solution is 1.7 mm for the ultramafic rocks. This value represents the initial displacement of the tunnel wall immediately after excavation. However, it's important to note that tunnel behavior is not solely governed by immediate displacements. Over time, the surrounding rock mass may continue to deform due to various factors such as stress redistribution, convergence, and long-term rock behavior (Soga et al., 2017). To account for these long-term effects, the long-term GRC is used. This curve takes into consideration the time-dependent behavior of the rock mass and predicts the final wall displacement (Oke et al., 2018a). In this case, the final wall displacement predicted by the long-term GRC is 2.55 mm as shown in Fig. 2. The tunnel convergence without support is 0.02% and the long-term final convergence is 0.029%. Fig. 3 shows the GRC curve using Duncan Fama solution. The tunnel wall displacement and Tunnel convergence in both of the solution is almost the same. The difference between the total wall displacement and the final wall displacement can be attributed to the time-dependent behavior of the rock mass. As time progresses, the rock mass continues to adjust and deform, resulting in additional displacement beyond the initial response. To explain this difference, it is emphasized that the Carranza-Torres solution provides an estimate of the immediate displacement, while the long-term GRC incorporates the time-dependent effects to estimate the final displacement. This accounts for the ongoing deformation

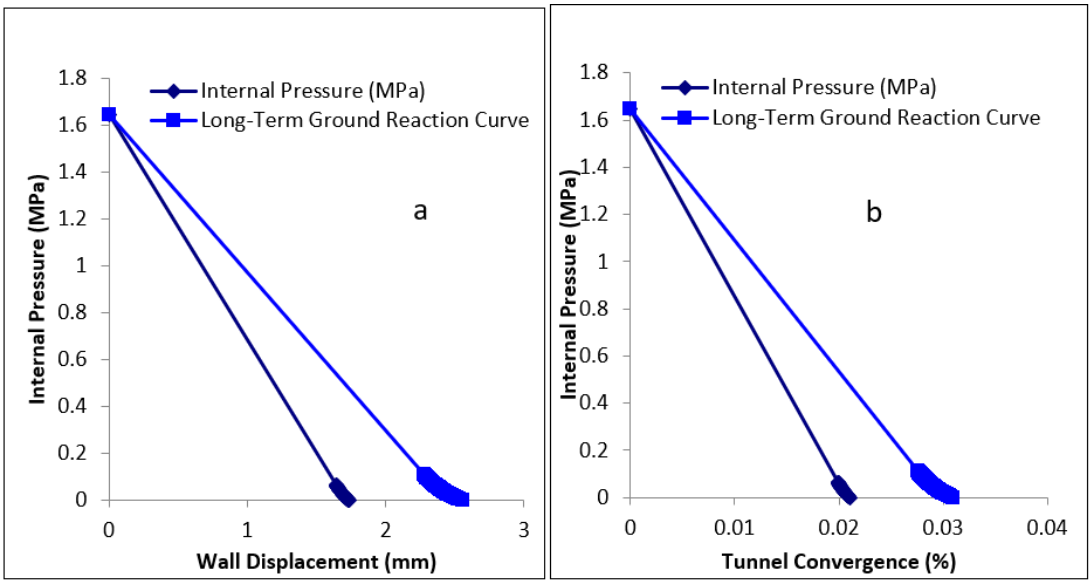

Figure 2. Ground reaction curve using Carranza-Torres solution for rock type B.

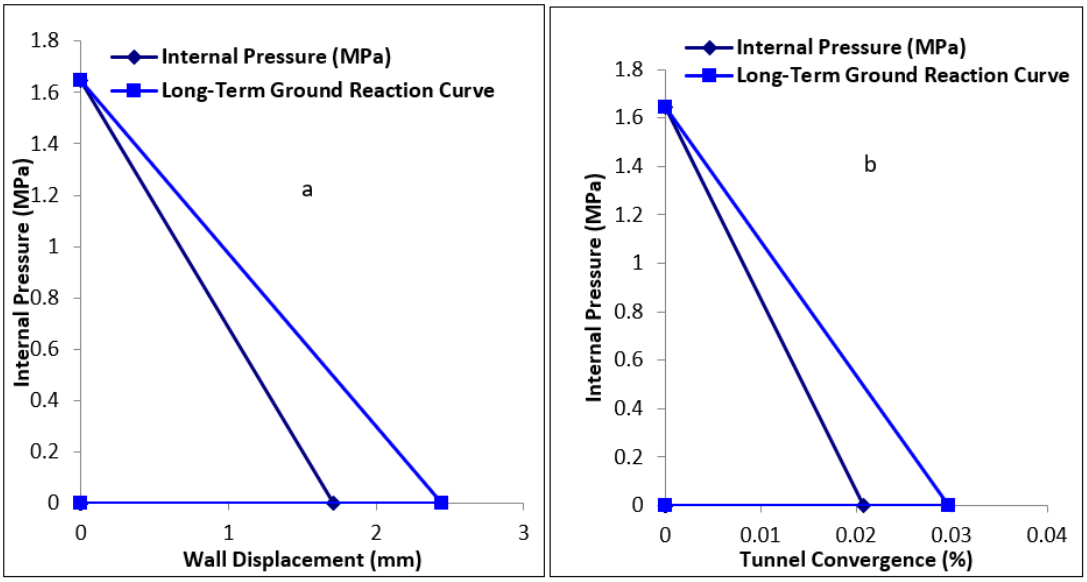

Figure 3. Ground reaction curve using Duncan Fama solution for rock type B.

and adjustment of the rock mass, leading to a larger displacement value in the long term. The stress environment of the surrounding rock changed during the tunnel excavation (Bao et al., 2022). These values are based on the assumptions and parameters used in the Carranza-Torres solution. Any uncertainties or variations in the rock mass properties, support system, or excavation method could impact the actual displacements experienced in the tunnel.

When a support is installed in the tunnel, it serves to reinforce the rock mass and limit its deformation. In this case, the Carranza-Torres solution predicts a reduction in displacement at the tunnel face to 0.5 mm and a displacement of 0.8 mm at the support level as shown in Fig. 4. The tunnel convergence refers to the inward movement or deformation of the tunnel walls due to excavation-induced stress redistribution. In this case, the Carranza-Torres solution predicts a convergence of 0.006% at the tunnel face and a convergence of 0.01% after installation of support. A convergence of 0.006% implies that the tunnel walls have moved by 0.006% of the tunnel diameter toward the center. This convergence occurs due to the redistribution of stresses and the response of the surrounding rock mass to excavation (Luc et al., 2015). The convergence at the support level represents the inward movement of the tunnel walls specifically near the installed support elements (Oke et al., 2018b). A convergence of 0.01% means that the walls have moved

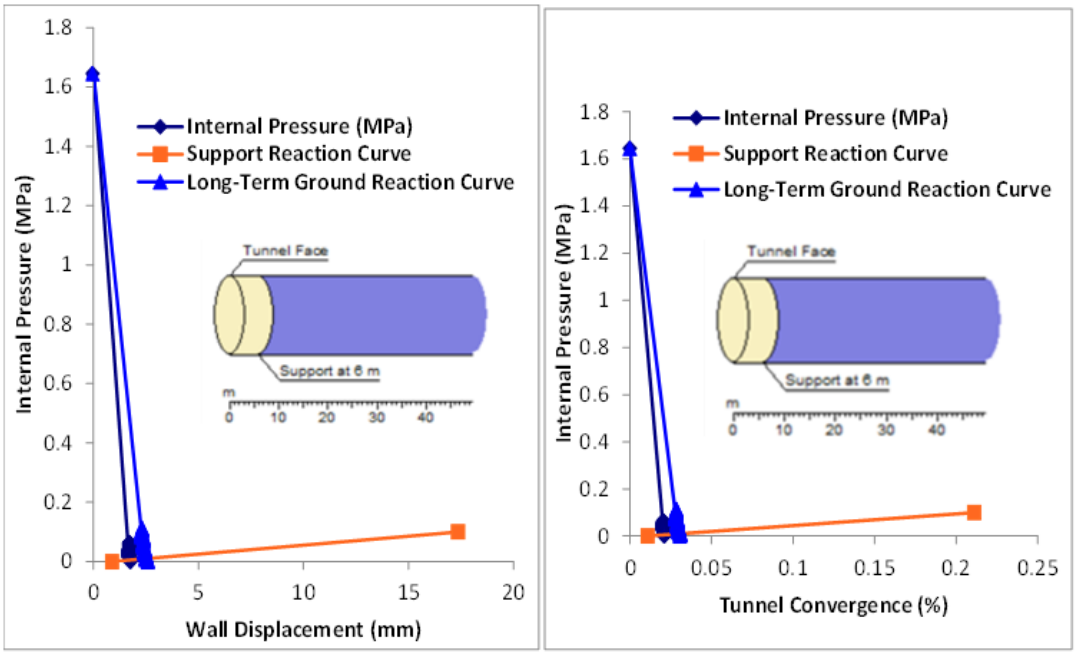

Figure 4. Ground reaction curve using Carranza-Torres solution after installing support for rock type B.

by 0.01% of the tunnel diameter towards the center at the support location. The installed support helps to limit the convergence and deformations by providing reinforcement and confinement to the rock mass. Fig. 5 shows the similar results using Duncan Fama solution.

The GRC for rock type A is given in Figs. 6 to 9. Without the installation of support (Figs. 6 and 7), the tunnel walls experience deformation due to the redistribution of stresses induced by excavation. The convergence in tunnel using the Carranza-Torres solution is 0.003% which indicates that the tunnel walls have moved by 0.003% of the tunnel diameter towards the center. This movement occurs as a result of the response of the surrounding rock mass to the excavation process. The estimation of 0.004% as the long-term final convergence suggests that the rock mass will experience further inward movement, resulting in an additional convergence of 0.004% of the tunnel diameter. When support is not installed, the tunnel walls undergo deformation due to the redistribution of stresses induced by excavation (Huang et al., 2020). The final wall displacement of 0.25 mm (Fig. 5) represents the total movement or deformation of the tunnel walls at the end of the excavation process. This displacement takes into account the immediate response of the rock mass to the excavation. The estimation of 0.36 mm (Fig. 7) as the long-term final wall displacement suggests that the rock mass will experience further movement or deformation, resulting in an additional displacement of 0.36 mm. While when support (Fig. 8) is installed the final wall displacement is reduced to 0.08 mm and the long-term final wall displacement is reduced to

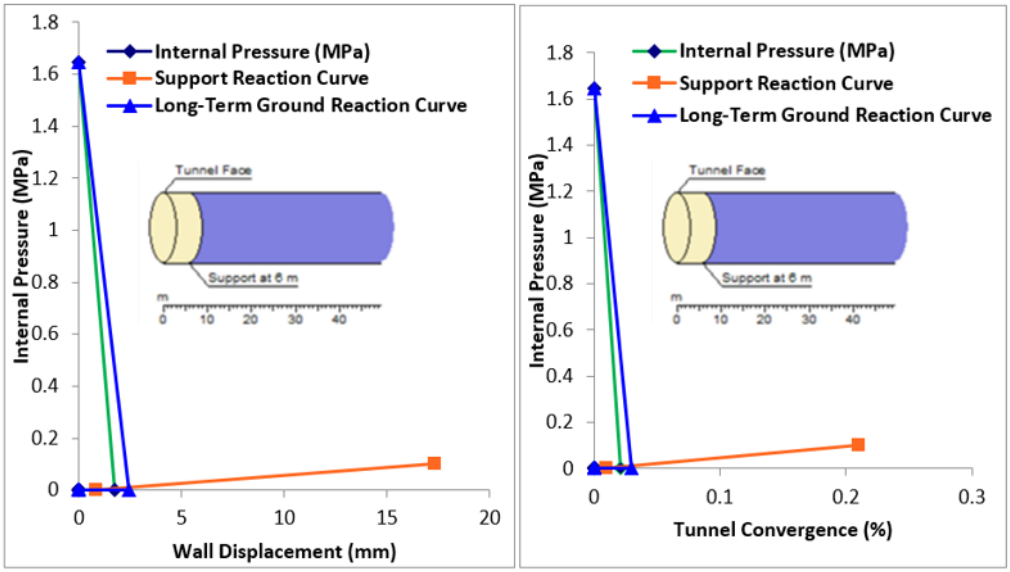

Figure 5. Ground reaction curve using Duncan Fama solution after installing support for rock type B.

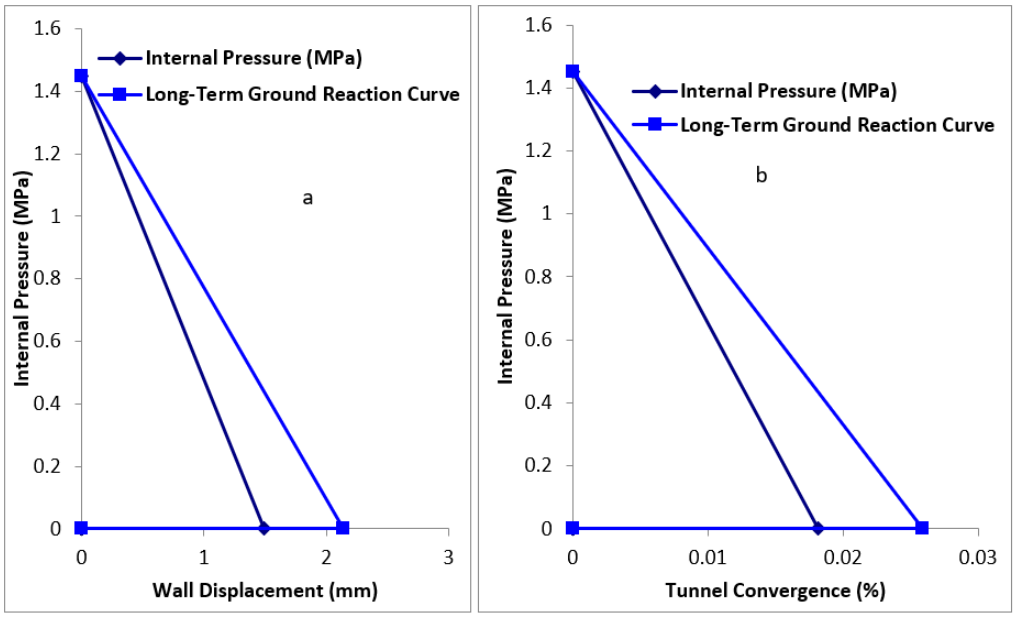

Figure 6. Ground reaction curve using Duncan Fama solution for rock type A.

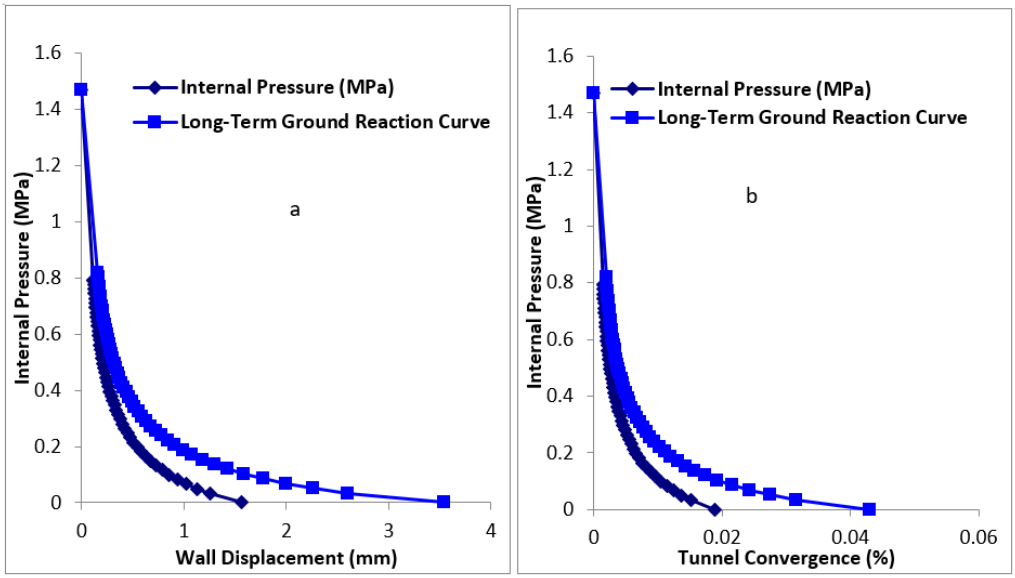

Figure 7. Ground reaction curve using Carranza-Torres solution before installation of support.

0.11 mm for Carranza-Torres solution. The support system helps to limit the merging and deformations by providing strengthening and confinement to the rock mass (Su et al., 2021).

The Duncan Fama solution (Fig. 9) indicated that after installing support the tunnel convergence is almost 0%, it means that there is no measurable inward movement or deformation of the tunnel walls. The support system, such as rock bolts, shotcrete, or steel ribs, effectively restrains the rock mass and prevents it from converging or collapsing inward (Ghorbani et al., 2020). A tunnel convergence of 0% indicates that the support system is successfully fulfilling its purpose of providing reinforcement and stability to the tunnel structure. The support elements distribute the loads and reinforce the rock mass, effectively counteracting the excavation-induced stresses and maintaining the integrity of the tunnel (Kaiser and Cai, 2012). However, it's important to note that a convergence value of 0% may be an ideal scenario and not always achievable in practice. The actual convergence may still exist but below the measurable threshold, indicating minimal or negligible movement. In such cases, continuous monitoring is necessary to ensure the stability of the tunnel and detect any potential convergence or deformations that may occur over time.

Finally, the total displacement across the tunnel cross section was also measured using Hoek-Brown parameters as shown in Fig. 10. It was observed that when the when the support is installed there is negligible displacement along

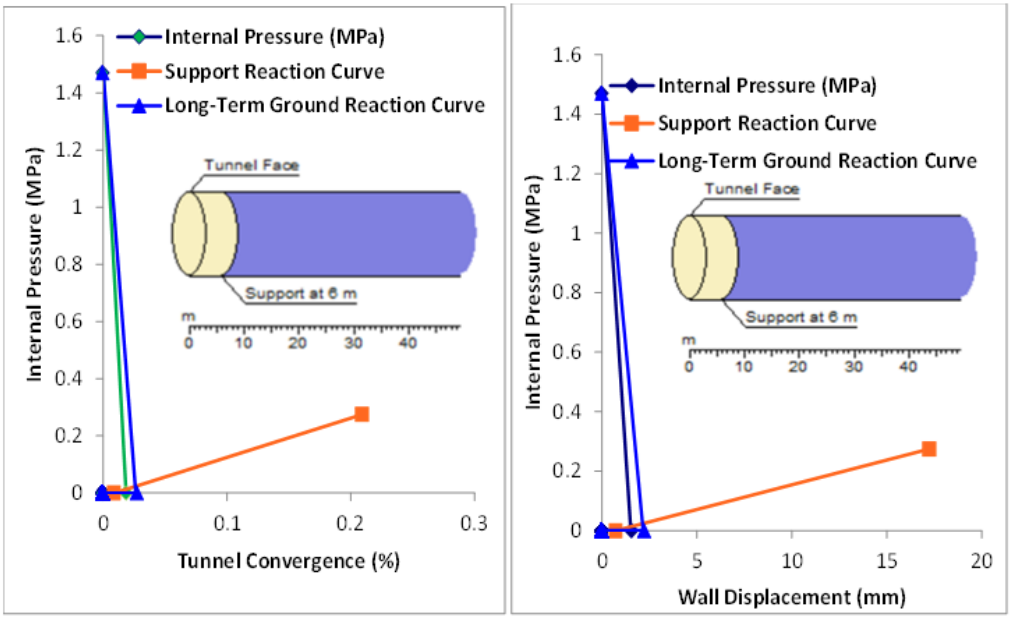

Figure 8. Ground reaction curve using Carranza-Torres solution after installing support.

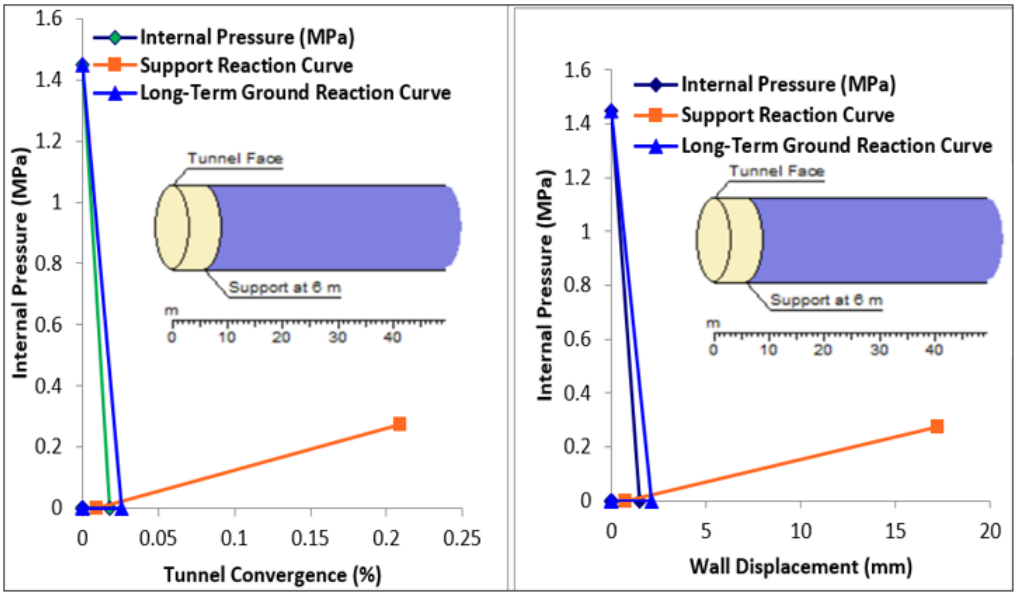

Figure 9. Ground reaction curve using Duncan Fama solution after installing support.

the tunnel crown and walls for both the rock types.

The pullout test results from the rock bolt installation in the tunneling project reveal a positive linear relationship between bolt stress and displacement, indicative of elastic deformation behavior. The bolt withstood a maximum stress of 346 MPa with only a slight displacement increase of 3.5 mm, highlighting its stability and validity of the installed support and numerical analysis results as discussed above. As load intensified from 20 kN to 206 kN, elastic deformation increased from 0.07 mm to 0.69 mm, demonstrating progressive load-bearing. Moreover, yield strength increased by 7% to 67%, showing enhanced capacity for heavier loads while staying within the elastic range. These results indicate the efficiency of the recommended support system (Bieniawski, 1989) for good and poor rock mass crucial for maintaining stability and safety amid challenging Himalayan geological conditions, providing valuable provision for future tunneling projects.

4. Conclusion

Monitoring the displacement of tunneling in jointed rock masses is crucial for ensuring tunnel stability. This study focused on calculating the field displacement of a tunneling project in the Himalayas, particularly in the tunnel's roof and walls. Both analytical and numerical methods were employed to calculate the displacement field. The objective was to measure the displacement occurring after excavation to guide the effective implementation and installation of support systems within the tunnel. The conclusion is given below:

- The numerical modeling approach revealed that, after installing the support, the total displacement across the

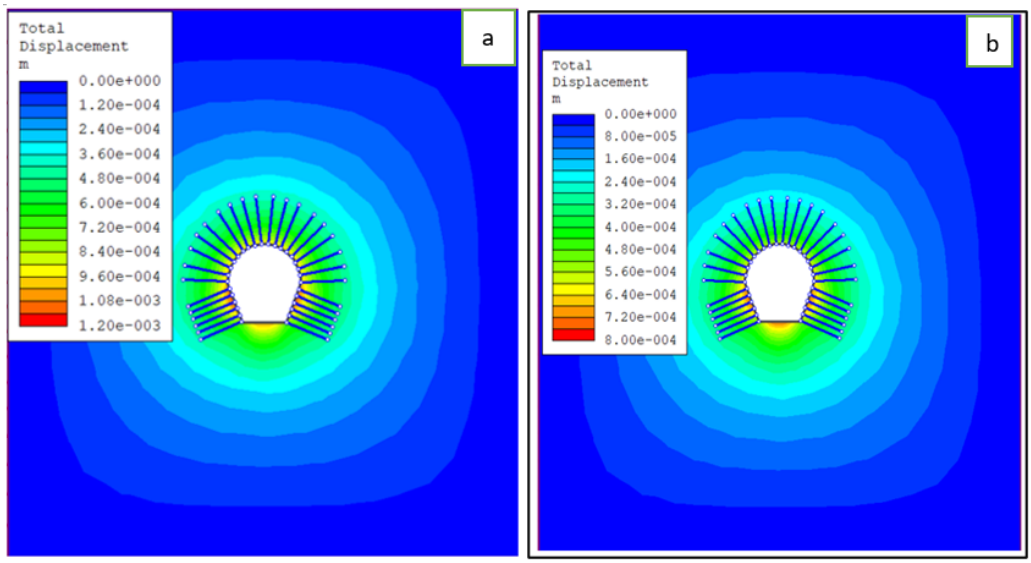

Figure 10. The displacement across tunnel for both rock types A and B.

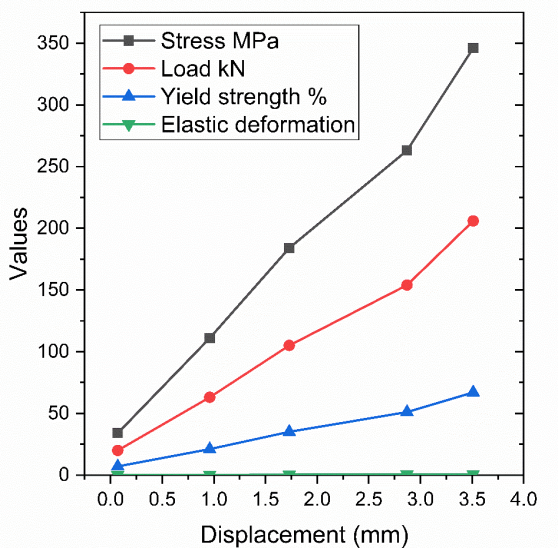

Figure 11. Stress on rock bolt vs displacement of rock bolt.

crown and wall was reduced to an allowable limit. This indicates the efficiency of the installed support and the suitability of the numerical analysis parameters and methods used.

- The Duncan Fama solution indicated that the installation of support in good rock mass resulted in almost 0% tunnel convergence, implying negligible inward movement or deformation of the tunnel walls. Conversely, the Carranza-Torres solution showed a convergence of 0.003%, indicating that the tunnel walls moved by 0.003% of the tunnel diameter towards the center. For poor rock mass, the Carranza-Torres solution predicted a convergence of 0.006% at the tunnel face and 0.01% at the support level. Additionally, a reduction in displacement at the tunnel face to 0.5 mm and a displacement of 0.8 mm at the support level were anticipated.

- Considering that the numerical modeling approach utilized the ground parameters to estimate wall displacement, it proved to be more suitable than analytical approaches. It is therefore recommended to validate the design support using numerical modeling rather than relying solely on analytical methods, taking into account the limitations associated with the ground conditions.

- The pullout test on the bolts indicated its elastic stress distribution and stability, underscored by the linear stress-displacement correlation and impressive yield strength increase. These results confirm the efficiency of the installed support for ensuring safety and performance in demanding geological contexts.

- The reliability of the results depends on the accurate ground parameters, field data validation, therefore future directions involve enhanced ground parameter collection, advanced and hybrid numerical modeling techniques, real-time monitoring integration, and long-term performance assessment to improve tunnel stability predictions and support system effectiveness.

Authors contributions
Authors have contributed equally in preparing and writing the manuscript.

Availability of data and materials
The data that support the findings of this study are available from the corresponding author, upon reasonable request.

Conflict of interests
The authors declare that they have no known competing financial interests or personal relationships that could have appeared to influence the work reported in this paper.

References

Abbas N., Li K. G., Abbas N., Ali R. (2022) Correlation of Schmidt Hammer rebound number and point load index with compressive strength of sedimentary, igneous and metamorphic rocks. *Journal of Mining Science* 58 (6): 903–910. DOI: https://doi.org/10.1134/S1062739122060047.

Abdollahi M. S., Najafi M., Bafghi A. Y., Marji M. F. (2019) A 3D numerical model to determine suitable reinforcement strategies for passing TBM through a fault zone, a case study: Safaroud water transmission tunnel, Iran. *Tunnelling and Underground Space Technology* 88:186–199. DOI: https://doi.org/10.1016/j.tust.2019.03.008.

Arif M., Islam I., Rizwan M. (2015) Petrography and physico-mechanical properties of the granitic rocks from Kumrat valley, Kohistan Batholith, NW Pakistan.

Bao H., Liu C., Liang N., Lan H., Yan C., Xu X. (2022) Analysis of large deformation of deep-buried brittle rock tunnel in strong tectonic active area based on macro and microcrack evolution. *Engineering Failure Analysis* 138:106351. DOI: https://doi.org/10.1016/j.engfailanal.2022.106351.

Bao H., Zhang K., Yan C., Lan H., Wu F., Zheng H. (2020) Excavation damaged zone division and time-dependency deformation prediction: A case study of excavated rock mass at Xiaowan Hydropower Station. *Engineering Geology* 272:105668. DOI: https://doi.org/10.1016/j.enggeo.2020.105668.

Bi J., Zhou X. P., Qian Q. H. (2016) The 3D numerical simulation for the propagation process of multiple pre-existing flaws in rock-like materials subjected to biaxial compressive loads. *Rock Mechanics and Rock Engineering* 49 (5): 1611–1627. DOI: https://doi.org/10.1007/s00603-015-0867-y.

Bieniawski Z. T. (1989) Engineering rock mass classifications: A complete manual for engineers and geologists in mining, civil, and petroleum engineering. John Wiley & Sons

Bobet A. (2010) Numerical methods in geomechanics. *The Arabian Journal for Science and Engineering* 35

Carranza-Torres C. (2004) Elasto-plastic solution of tunnel problems using the generalized form of the Hoek-Brown failure criterion. *International Journal of Rock Mechanics and Mining Sciences* 41:629–639. DOI: https://doi.org/10.1016/j.ijrmms.2004.03.111.

Carranza-Torres C., Fairhurst C. (2000) Application of the Convergence-Confinement method of tunnel design to rock masses that satisfy the Hoek-Brown failure criterion. *Tunnelling and Underground Space Technology* 15 (2): 187–213. DOI: https://doi.org/10.1016/S0886-7798(00)00046-8.

——— (1999) The elasto-plastic response of underground excavations in rock masses that satisfy the Hoek-Brown failure criterion. *International Journal of Rock Mechanics and Mining Sciences* 36 (6): 777–809. DOI: https://doi.org/10.1016/S0148-9062(99)00047-9.

Dehghan A. N., Yazdi A. (2023) A geomechanical investigation for optimizing the ultimate slope design of Shadan Open Pit Mine, Iran. *Indian Geotechnical Journal,* 1–15. DOI: https://doi.org/10.1007/s40098-022-00709-w.

Fama M. E. D. (1993) Numerical modeling of yield zones in weak rock. In *Analysis and Design Methods,* edited by Fairhurst C., 49–75. Oxford: Pergamon

Furtney J., Thielsen C., Fu W., Le G. R. (2022) Surrogate models in rock and soil mechanics: Integrating numerical modeling and machine learning. *Rock Mechanics and Rock Engineering,* 1–15. DOI: https://doi.org/10.1007/s00603-021-02720-8.

Ghorbani M., Shahriar K., Sharifzadeh M., Masoudi R. (2020) A critical review on the developments of rock support systems in high stress ground conditions. *International Journal of Mining Science and Technology* 30 (5): 555–572. DOI: https://doi.org/10.1016/j.ijmst.2020.06.002.

Hoek E. (2018) Support for very weak rock associated with faults and shear zones. *Rock Support and Reinforcement Practice in Mining*

Hoek E., Carranza-Torres C., Corkum B. (2002) Hoek-Brown failure criterion-2002 edition. *Proceedings of NARMS-Tac* 1 (1): 267–273.

Hoek E., Diederichs M. S. (2006) Empirical estimation of rock mass modulus. *International Journal of Rock Mechanics and Mining Sciences* 43 (2): 203–215. DOI: https://doi.org/10.1016/j.ijrmms.2005.06.005.

Huang F., Zhang M., Wang F., Ling T., Yang X. (2020) The failure mechanism of surrounding rock around an existing shield tunnel induced by an adjacent excavation. *Computers and Geotechnics* 117:103236. DOI: https://doi.org/10.1016/j.compgeo.2019.103236.

Ji M., Wang X., Luo M., Wang D., Teng H., Du M. (2023) Stability analysis of tunnel surrounding rock when TBM passes through fracture zones with different deterioration levels and dip angles. *Sustainability* 15 (6) DOI: https://doi.org/10.3390/su15065243.

Jing L., Hudson J. A. (2002) Numerical methods in rock mechanics. *International Journal of Rock Mechanics and Mining Sciences* 39 (4): 409–427. DOI: https://doi.org/10.1016/S1365-1609(02)00065-5.

Kabwe E., Karakus M., Chanda E. K. (2020) Proposed solution for the ground reaction of non-circular tunnels in an elastic-perfectly plastic rock mass. *Computers and Geotechnics* 119:103354. DOI: https://doi.org/10.1016/j.compgeo.2019.103354.

Kaiser P. K., Cai M. (2012) Design of rock support system under rockburst condition. *Journal of Rock Mechanics and Geotechnical Engineering* 4 (3): 215–227. DOI: https://doi.org/10.3724/SP.J.1235.2012.00215.

Karimiazar J., Sharifi Teshnizi E., O'Kelly B. C., Sadeghi S., Karimizad N., Yazdi A., Arjmandzadeh R. (2023) Effect of nano-silica on engineering properties of lime-treated marl soil. *Transportation Geotechnics* 43:101123. DOI: https://doi.org/10.1016/j.trgeo.2023.101123.

KC D., Gautam K., Dangi H., Kadel S., Hu L. (2022) Challenges in tunneling in the Himalayas: A survey of several prominent excavation projects in the Himalayan mountain range of South Asia. *Geotechnics,* DOI: https://doi.org/10.3390/geotechnics2040039.

Lan H., Chen J., Macciotta R. (2019) Universal confined tensile strength of intact rock. *Scientific Reports* 9 (1): 6170. DOI: https://doi.org/10.1038/s41598-019-42698-6.

Li P., Wang K., Li X., Lu D. (2014) Analytical solutions of a finite two-dimensional fluid-saturated poroelastic medium with compressible constituents. *International Journal for Numerical and Analytical Methods in Geomechanics* 38 (11): 1183–1196. DOI: https://doi.org/10.1002/nag.2255.

Liu L., Xu C., Du X., Iqbal K. (2023) Longitudinal seismic response of shield tunnel: A multi-scale numerical analysis. *Tunnelling and Underground Space Technology* 138:105163. DOI: https://doi.org/10.1016/j.tust.2023.105163.

Luc L. M., Ndop J., Ndjaka J. (2015) Numerical investigations of stresses and strains redistribution around the tunnel: Influence of transverse isotropic behavior of granitic rock, in situ stress and shape of tunnel. *Journal of Mining Science* 51:497–505. DOI: https://doi.org/10.1134/S1062739115030102.

Oke J., Vlachopoulos N., Diederichs M. (2018a) Improvement to the convergence-confinement method: Inclusion of support installation proximity and stiffness. *Rock Mechanics and Rock Engineering* 51 DOI: https://doi.org/10.1007/s00603-018-1418-0.

——— (2018b) Improvement to the convergence-confinement method: Inclusion of support installation proximity and stiffness. *Rock Mechanics and Rock Engineering* 51 (5): 1495–1519. DOI: https://doi.org/10.1007/s00603-018-1418-0.

Paltrinieri E., Sandrone F., Zhao J. (2016) Analysis and estimation of gripper TBM performances in highly fractured and faulted rocks. *Tunnelling and Underground Space Technology* 52:44–61. DOI: https://doi.org/10.1016/j.tust.2015.11.017.

Petterson M. (2010) A Review of the geology and tectonics of the Kohistan island arc, north Pakistan. *Geological Society of London Special Publications* 338:287–327. DOI: https://doi.org/10.1144/SP338.14.

Singh G. S. P., Singh U., Murthy V. (2010) Applications of numerical modelling for strata control in mines. *Geotechnical and Geological Engineering* 28:513–524. DOI: https://doi.org/10.1007/s10706-010-9324-6.

Soga K., Laver R. G., Li Z. (2017) Long-term tunnel behaviour and ground movements after tunnelling in clayey soils. *Underground Space* 2 (3): 149–167. DOI: https://doi.org/10.1016/j.undsp.2017.08.001.

Su Y., Su Y., Zhao M., Vlachopoulos N. (2021) Tunnel stability analysis in weak rocks using the convergence confinement method. *Rock Mechanics and Rock Engineering* 54 (2): 559–582. DOI: https://doi.org/10.1007/s00603-020-02304-y.

Wang Y., Zhou X., Shou Y. (2017) The modeling of crack propagation and coalescence in rocks under uniaxial compression using the novel conjugated bond-based peridynamics. *International Journal of Mechanical Sciences* 128-129:614–643. DOI: https://doi.org/10.1016/j.ijmecsci.2017.05.019.

Wang Y., Zhou X., Wang Y., Shou Y. (2018) A 3-D conjugated bond-pair-based peridynamic formulation for initiation and propagation of cracks in brittle solids. *International Journal of Solids and Structures* 134:89–115. DOI: https://doi.org/10.1016/j.ijsolstr.2017.10.022.

Wang Y., Zhou X., Xu X. (2016) Numerical simulation of propagation and coalescence of flaws in rock materials under compressive loads using the extended non-ordinary state-based peridynamics. *Engineering Fracture Mechanics* 163:248–273. DOI: https://doi.org/10.1016/j.engfracmech.2016.06.013.

Yang B., Mitelman A., Elmo D., Stead D. (2021) Why the future of rock mass classification systems requires revisiting their empirical past. *Quarterly Journal of Engineering Geology and Hydrogeology* 55

Yao W. W., Zhou X. P., Qian Q. H. (2022) From statistical mechanics to nonlocal theory. *Acta Mechanica* 233 (3): 869–887. DOI: https://doi.org/10.1007/s00707-021-03123-0.

Zhao K., Janutolo M., Barla G., Chen G. (2014) 3D simulation of TBM excavation in brittle rock associated with fault zones: The Brenner Exploratory Tunnel case. *Engineering Geology* 181:93–111. DOI: https://doi.org/10.1016/j.enggeo.2014.07.002.

Zhou H., Gao Y., Zhang C., Yang F., Hu M., Liu H., Jiang Y. (2018) A 3D model of coupled hydro-mechanical simulation of double shield TBM excavation. *Tunnelling and Underground Space Technology* 71:1–14. DOI: https://doi.org/10.1016/j.tust.2017.07.012.

Zhou X. P., Bi J., Qian Q. H. (2015) Numerical simulation of crack growth and coalescence in rock-like materials containing multiple pre-existing flaws. *Rock Mechanics and Rock Engineering* 48 (3): 1097–1114. DOI: https://doi.org/10.1007/s00603-014-0627-4.

Zhou X. P., Yang H. Q. (2012) Multiscale numerical modeling of propagation and coalescence of multiple cracks in rock masses. *International Journal of Rock Mechanics and Mining Sciences* 55:15–27. DOI: https://doi.org/10.1016/j.ijrmms.2012.06.001.

Zhou Y., Teo T., Cai J. (2017) Rock engineering practice for development of underground caverns in Singapore.

Öge I. (2017) Assessing rock mass permeability using discontinuity properties. *Procedia Engineering* 191:638–645. DOI: https://doi.org/10.1016/j.proeng.2017.05.373.